Quantum noise and squeezing in an optical parametric oscillator with arbitrary output-mirror coupling

Bartram S. Abbott and Sudhakar Prasad
Department of Physics and Astronomy, University of New Mexico, Albuquerque, New Mexico 87131
and Center for Advanced Studies, University of New Mexico, Albuquerque, New Mexico 87131
(Received 10 June 1991)

We consider here the problem of quantum noise in light produced by an optical parametric oscillator operating below threshold inside a single-sided cavity. By employing the correct boundary conditions on quantum fields at the output mirror, a procedure that is valid for *arbitrary* mirror transmission, we derive exact expressions for quantum-noise reduction for arbitrary pump phase and output-mirror coupling. We find that for a given output-mirror power reflectance R, squeezing of quantum noise in the intracavity field increases to a final fractional value equal to $R/(1+R)$ as the pump intensity is increased and the oscillation threshold is approached. The output field, on the other hand, exhibits perfect squeezing of noise in one quadrature of its central Fourier component at threshold regardless of the output-mirror coupling. The present approach, which is based on boundary conditions, is quite general and applicable to any matter-field interaction problem inside a cavity.

PACS number(s): 42.50.Lc, 42.50.Dv, 42.65.Ky

I. INTRODUCTION

During the past decade, the usefulness of a degenerate parametric oscillator in producing squeezed states [1] has been demonstrated. However, Milburn and Walls [2] showed that the maximum intracavity squeezing obtained from such an oscillator is 50%, not nearly enough to offer any great advantage in the proposed uses of squeezed light. Consequently, the role of the degenerate parametric oscillator as a useful squeezing device would have been deemed minimal were it not for the work of Yurke [3], who discovered that the squeezing in the output field is not the same as the squeezing of the intracavity field. Indeed, the noise reduction outside the cavity may actually be much larger than that inside the cavity. This has led to further studies by Collett, Gardiner, and Savage [4], and also by Carmichael [5], who discussed the connection between intracavity quantum fluctuations and the measured squeezing at an outside detector. More recently, one of the authors and co-workers [6] have considered the relationship between single-quasimode squeezing of the intracavity field and spectral squeezing of the input and output fields in a manner that emphasizes the physical nature of the relationship.

Although the formalism used in that work is fairly general in scope, the authors nevertheless applied it only to cavities with nearly perfectly reflecting output mirrors, thereby minimizing the coupling of the cavity to the outside. Gardiner and Savage [4] also started out with a general formalism, but then quickly specialized to the case of a nearly perfect cavity when computing the explicit expressions for squeezing. The present work seeks to offer further insight into the subject of squeezing by examining its dependence on the output-mirror transmission. The output mirror acts as a boundary between intracavity and extracavity fields. As mentioned before, in the good-cavity limit, there can exist a great variation in the degree of squeezing on either side of this boundary. However, this inside-outside dichotomy must diminish —and indeed disappear—as the mirror transmission rises to unity. In this limit, the mirror effectively disappears. A proper treatment of this inside-outside connection problem in cavities with arbitrary output coupling is the subject of the present paper, in which for definiteness we have treated the case of a degenerate parametric oscillator below threshold.

The problem dealt with here is not merely an intellectual exercise for an important class of devices, the semiconductor diode lasers [7], for which the output coupling can be quite large. One can imagine the production of squeezing by doping the diode with a nonlinear material.

It is also worth emphasizing that the approach of boundary conditions employed in this paper is perfectly general and applicable to any matter-field interaction inside a cavity. In fact, this approach has already been used by one of us to address the intrinsic linewidth of a laser [8] for arbitrary output-mirror transmission both above and below threshold.

Of pivotal importance to cavity quantum optics is the concept of quasimodes [9]. If there is indeed to be any output from a cavity, the finite transmittivity of the output mirror results in the quasimodes acquiring a finite linewidth. For high-Q cavities, this linewidth may be quite small compared to the frequency separation of successive quasimodes, allowing one to consider a quasimode as a single mode with a finite linewidth. However, as it is our goal to consider arbitrary mirror transmissions, this single-mode treatment is not sufficient since the linewidth of each quasimode is no longer negligible when the mirror transmittivity becomes large. An effort to quantize the intracavity field independently of the outside field as is commonly done for a good cavity is entirely incorrect

in this same limit for which the distinction between the two fields is completely obliterated.

An approach to cavity quantum optics that adequately corrects these shortcomings was first considered by Lang, Scully, and Lamb [10,11] and later by Ujihara [12]. Here the leaky cavity under consideration is enclosed within a larger cavity having perfectly reflecting walls. We shall henceforth call this larger cavity the "universe," its length eventually taken to approach infinity. In this way, the modes of the larger cavity (modes of the universe) can be properly and rigorously defined and the various fields inside and outside the leaky cavity can be considered as superpositions of these universe modes. In Refs. [10] and [11], the output mirror of the leaky cavity was represented by a δ-function dielectric bump. Subsequent work in Ref. [6] replaced the dielectric bump by a true mirror.

This paper shall proceed as follows. Section II will include a review of the modes of the universe following the notation of Ref. [6] closely. In Sec. III, the nonlinear parametric medium will be added to the previously empty cavity and the Hamiltonian and equation of motion for the universe mode operators will be derived. The fields will be separated into their right- and left-traveling pieces and their respective equations of motion will be found. In Sec. IV, we shall employ the boundary conditions to transform these equations to single-round-trip difference equations in order to reveal the effect of a single round trip through the cavity. Variances will then be calculated and the intracavity squeezing determined. In Sec. V, we shall look at the spectral squeezing of the output field. The conclusions and outlook of this work will be presented in Sec. VI.

II. REVIEW OF THE UNIVERSE MODES

Our one-dimensional universe is represented by a large, empty cavity enclosed between two perfectly reflecting mirrors at positions $z=-L$ and l, as shown in Fig. 1. Located at $z=0$ is a mirror of finite transmittivity. The leaky, physical, single-output-end cavity is between the mirrors at $z=0$ and l, while the perfect mirror at $z=-L$ is merely a mathematical construct that must be taken away by setting $L=\infty$ before any physically meaningful statements can be made. For fields normally incident from the left, the output mirror at $z=0$ is described by real amplitude reflection and transmission coefficients $\tilde{r}$ and $\tilde{t}=(1-\tilde{r}^2)^{1/2}$. For fields normally incident from the right, these become $-\tilde{r}$ and $\tilde{t}$.

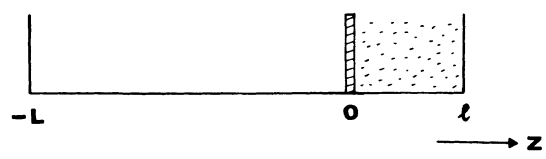

FIG. 1. Leaky cavity bounded by a perfectly reflecting mirror at $z=l$ and a partially transmitting mirror at $z=0$. The auxiliary cavity that along with the leaky cavity constitutes the universe is bounded by a perfectly reflecting mirror at $z=-L$ ($L\rightarrow\infty$) and the mirror at $z=0$.

Let $U_k(z)$ represent the electric-field amplitude at the frequency $\Omega_k=ck$. The boundary conditions at the perfect mirrors at $z=-L$ and l, namely that the fields must identically vanish there, dictate the following form for $U_k(z)$:

$$U_k(z)=\begin{cases}\xi_k\sin[k(z+L)] & \text{for } z<0\\ M_k\sin[k(z-l)] & \text{for } z>0\ .\end{cases} \tag{2.1}$$

In addition, the boundary conditions at the leaky mirror at $z=0$ imply a discrete set of allowed values of k, separated one from the next by $\Delta k=\pi/L$ in the limit $L\gg l$. They also determine the ratio of M_k and ξ_k. By letting ξ_k alternate between 1 and -1 as k increases, we may show that [6]

$$M_k=\left[\frac{p}{p^2\cos^2 kl+\sin^2 kl}\right]^{1/2},\quad p=\frac{1-\tilde{r}}{1+\tilde{r}}\ , \tag{2.2}$$

which is a periodically peaked function of k. In the good-cavity limit $\tilde{r}\rightarrow 1$, the behavior of M_k^2 around each peak may be approximated by the usual Lorentzian form with half-width at full maximum $(1-\tilde{r})/2l$.

Different modes $\{U_k\}$ are orthogonal and therefore rigorously independent. We may therefore quantize the electric field of radiation in terms of these modes of the universe:

$$\begin{aligned}E(z,t)&=E^{(+)}(z,t)+E^{(-)}(z,t)\\&=\sum_k\left[\frac{\hbar\Omega_k}{\epsilon_0 AL}\right]^{1/2}a_k(t)U_k(z)+\text{H.c.}\ ,\end{aligned} \tag{2.3}$$

where a_k are the universe mode annihilation operators defining the positive frequency part $E^{(+)}(z,t)$ of the field in the Heisenberg picture and A is the cross-sectional area of the cavity. We can identify *intracavity* and *extracavity* fields by considering the regions $z>0$ and $z<0$, respectively. Inside the leaky cavity of interest, $z>0$, it is the periodically peaked behavior of M_k's that defines the cavity quasimode structure, the width of each peak being determined by the reflectivity $\tilde{r}$. Thus, for instance, the positive frequency component of the intracavity field is given by

$$E^{(+)\text{cav}}(z,t)=\sum_k\left[\frac{\hbar\Omega_k}{\epsilon_0 AL}\right]^{1/2}M_k a_k\sin[k(z-l)]\ . \tag{2.4}$$

This field can further be separated into its right- and left-traveling pieces by writing $\sin[k(z-l)]$ as a difference of two exponentials. This separation is necessary, since not only are the boundary conditions specifically dependent on these particular fields, but also the output of the cavity is related to the transmitted part of the left-traveling field alone. If $e_+(z,t)$ and $e_-(z,t)$ denote the envelopes of the right- and left-traveling fields,

$$E^{(+)\text{cav}}(z,t)\equiv[e_+(z,t)e^{ik_0 z}+e_-(z,t)e^{-ik_0 z}]e^{-i\Omega_0 t}\ , \tag{2.5}$$

then in terms of slowly varying mode amplitudes A_k

defined by $a_k = A_k e^{-i\Omega_0 t}$, we have

$$e_{\pm}(z,t) = \pm \frac{1}{2i} \sum_k \left[\frac{\hbar \Omega_k}{\epsilon_0 AL} \right]^{1/2} M_k A_k e^{\pm i \delta \Omega_k z/c} e^{\mp ikl} , \tag{2.6}$$

in which $\delta\Omega_k \equiv \Omega_k - \Omega_0$ is the frequency detuning of the a_k mode from the central universe mode.

This review demonstrates how the electric fields inside and outside a one-sided empty cavity having an arbitrary output transmission may be properly constructed. An extension of these concepts to double-sided cavities is straightforward. These expressions provide the tools with which the parametric oscillator may now be examined for cavities of arbitrary quality.

III. DEGENERATE PARAMETRIC OSCILLATOR

A degenerate parametric oscillator squeezes optical fields via the second-order nonlinearity $\chi^{(2)}$. Very simply, through the nonlinear interaction, each photon of a pump field of frequency $2\Omega_0$ can generate two photons of frequency Ω_0, and conversely two photons of frequency Ω_0 can combine into a single photon of frequency $2\Omega_0$. It is the light at frequency Ω_0 that is squeezed via this interaction. Although the basis of this nonlinearity is microscopic and as such a full microscopic matter-field treatment is called for, we shall be content here with only an effective-Hamiltonian treatment in which the atomic system has been eliminated in an approximate way. The Hamiltonian for such a process may be written as [13,14]

$$H = \tfrac{1}{2} \int_{\text{universe}} [\epsilon(\mathbf{r}) E^2(\mathbf{r},t) + \mu_0 H^2(\mathbf{r},t)] d\mathbf{r} . \tag{3.1}$$

Assuming only a $\chi^{(2)}$ nonlinearity, we may expand $\epsilon(\mathbf{r})$ as $\epsilon(\mathbf{r}) = \epsilon_0 + \chi^{(2)} E(\mathbf{r},t)$. In view of this nonlinearity, the full Hamiltonian H can be split up into the usual unperturbed Hamiltonian H_0 and an interaction term H' arising purely from the nonlinearity

$$H' = \frac{A}{2} \chi^{(2)} \int_{\text{cavity}} E^{\text{cav}^3}(z,t) dz , \tag{3.2}$$

where it has been assumed for simplicity that the electric field has no transverse x-y dependence. Note that the integration in (3.2) is now confined to the nonlinear medium. The electric field $E^{\text{cav}}(z,t)$ includes both the quantized field (populated by photons in modes centered in frequency at Ω_0) as well as the pump field, which is assumed to be intense and therefore treatable classically. One may then write

$$E^{\text{cav}}(z,t) = E^{\text{cav}}_{\text{quantum}}(z,t) + E^{\text{cav}}_{\text{pump}}(z,t) . \tag{3.3}$$

Substitution of Eq. (3.3) into Eq. (3.2) generates several terms, but the particular nonlinear process of interest, namely the conversion of one pump photon into two signal photons and vice versa, is described by only one of these terms. We ignore all other terms as being of no value here, which amounts to the following replacement in the integral (3.2):

$$E^{\text{cav}^3}(z,t) \rightarrow 3 E^{\text{cav}}_{\text{pump}}(z,t) E^{\text{cav}^2}_{\text{quantum}}(z,t) .$$

Rewriting the pump field as

$$\frac{3A}{2} \chi^{(2)} E^{\text{cav}}_{\text{pump}}(z,t) \equiv \frac{i\hbar}{2} Q(z) e^{-2i\Omega_0 t} + \text{c.c.} , \tag{3.4}$$

splitting $E^{\text{cav}}_{\text{quantum}}(z,t)$ into its positive and negative frequency components, and neglecting fast varying terms, we may reexpress the full Hamiltonian H as

$$H = H_0 + \frac{i\hbar}{2} e^{-2i\Omega_0 t} \int_{\text{cavity}} Q(z') E^{(-)^2}(z',t) dz' + \text{H.c.} \tag{3.5}$$

The "cavity" and "quantum" designations have been dropped for simplicity. By using this Hamiltonian, we may write down the equation of motion for the universe mode annihilation operator a_k and hence for its slowly varying amplitude A_k:

$$\frac{dA_k}{dt} = -i\delta\Omega_k A_k + M_k \left[\frac{\hbar \Omega_k}{\epsilon_0 AL} \right]^{1/2} \int_0^l dz' Q(z') \sin[k(z'-l)] E^{(-)}(z',t) . \tag{3.6}$$

By operating on Eq. (2.6) by $(\partial/\partial z \pm \partial/c\partial t)$ and employing Eq. (3.6), we may show that

$$\left[\frac{\partial}{\partial z} \pm \frac{1}{c} \frac{\partial}{\partial t} \right] e_{\pm}(z,t) = \int_0^l Q(z') E^{(-)}(z',t) G_{\pm}(z,z') dz' , \tag{3.7}$$

where in our slowly varying amplitude approximation the functions $G_{\pm}(z,z')$ are given by the definitions

$$G_{\pm}(z,z') = \frac{\hbar \Omega_0}{2ic\epsilon_0 AL} \sum_k M_k^2 \sin[k(z'-l)] e^{\pm i \delta\Omega_k z/c} e^{\mp ikl} . \tag{3.8}$$

Due to the periodic behavior of M_k^2, one may show that the functions $G_{\pm}(z,z')$ consist of infinite sums of Dirac δ functions. For the physical situation $z,z' < l$, only one δ function in each sum contributes. So, as shown in detail in Appendix A, one effectively has

$$G_{\pm}(z,z') = \pm \frac{\hbar \Omega_0}{2\epsilon_0 Ac} \delta(z-z') e^{\mp ik_0 z} \quad \text{for } z,z' < l . \tag{3.9}$$

Since the right-hand side of Eq. (3.7) still contains the full field, it is now divided into its right- and left-traveling pieces. Recalling that $Q(z)$ contains the generally complex nonlinear susceptibility as well as the z-dependent part of the pump field, it too is broken up into right- and

left-traveling pieces. We let

$$Q(z)=qe^{i\theta_\chi}\sin(2k_0z+\phi)\frac{4\epsilon_0 Ac}{\hbar\Omega_0}\ , \tag{3.10}$$

where θ_χ is simply related to the phase of $\chi^{(2)}$ and ϕ is a phase shift of the pump field resulting either from propagation or from some other phase-shifting element. We shall have more to say about the importance of the phase shift ϕ later. Again neglecting fast varying terms, we arrive at the following equation of motion for $e_\pm(z,t)$:

$$\left[\frac{\partial}{\partial z}\pm\frac{1}{c}\frac{\partial}{\partial t}\right]e_\pm(z,t)=qe^{i\phi_\pm}e_\pm^\dagger(z,t),\quad \phi_\pm=\theta_\chi\pm\phi\ . \tag{3.11}$$

As expected, in the simple case of no nonlinear medium, $q=0$, these equations reduce to those for a freely propagating field.

The solution of Eqs. (3.11) proceeds as follows. Since these equations couple fields to their adjoints in a linear fashion, one may rewrite them in an explicitly decoupled form by constructing appropriate linear combinations of fields with their adjoints. These linear combinations, the so-called field quadratures, are the following:

$$X_\pm(z,t)=\frac{e_\pm(z,t)e^{-i\phi_\pm/2}+e_\pm^\dagger(z,t)e^{i\phi_\pm/2}}{2}\ , \tag{3.12a}$$

$$Y_\pm(z,t)=\frac{e_\pm(z,t)e^{-i\phi_\pm/2}-e_\pm^\dagger(z,t)e^{i\phi_\pm/2}}{2i}\ . \tag{3.12b}$$

In terms of the quadratures $X_\pm$ and $Y_\pm$, Eqs. (3.11) become

$$\left[\frac{\partial}{\partial z}\pm\frac{1}{c}\frac{\partial}{\partial t}\right]X_\pm(z,t)=qX_\pm(z,t)\ , \tag{3.13a}$$

$$\left[\frac{\partial}{\partial z}\pm\frac{1}{c}\frac{\partial}{\partial t}\right]Y_\pm(z,t)=-qY_\pm(z,t)\ . \tag{3.13b}$$

Equations (3.13) may be reformulated more simply in terms of the retarded times $\tau_+=t-z/c$ (for the e_+ field) and $\tau_-=t-(l-z)/c$ (for the e_- field). The resulting equations may be solved in terms of simple exponentials, which causally relate the right-traveling field quadratures and the left-traveling field quadratures to their values at the partially transmitting mirror and at the perfect mirror, respectively. One may show in this way that

$$\begin{aligned}
&X_+(z,t)=e^{qz}X_+(0,t-z/c)\ ,\\
&X_-(z,t)=e^{q(z-l)}X_-[l,t-(l-z)/c]\ ;\\
&Y_+(z,t)=e^{-qz}Y_+(0,t-z/c)\ ,\\
&Y_-(z,t)=e^{-q(z-l)}Y_-[l,t-(l-z)/c]
\end{aligned} \tag{3.14}$$

indeed satisfy Eqs. (3.13).

IV. BOUNDARY CONDITIONS AND SQUEEZING OF THE INTRACAVITY FIELD

Equations (3.14) reveal how the various quadratures evolve during a single rightward or leftward pass through the medium. The boundary conditions at the mirrors couple the left- and right-traveling fields and thereby enable us to determine the effect of propagation on either traveling field through an entire round trip. The π phase shift at the perfect mirror gives rise to a boundary condition for the fields:

$$e_+(l,t)=-e_-(l,t)\ . \tag{4.1a}$$

This implies, via definitions (3.12), the following matrix relationship between the field quadratures at the perfect mirror:

$$\begin{bmatrix}X_+(l,t)\\Y_+(l,t)\end{bmatrix}=\begin{bmatrix}-\cos\phi & -\sin\phi\\ \sin\phi & -\cos\phi\end{bmatrix}\begin{bmatrix}X_-(l,t)\\Y_-(l,t)\end{bmatrix}\ . \tag{4.1b}$$

At the output mirror, the right-traveling wave consists of the reflected part of the left-traveling wave and the transmitted vacuum field coming from outside the cavity:

$$e_+(0,t)=-\tilde{r}e_-(0,t)+\tilde{t}e^{\rm vac}(0,t)\ , \tag{4.2a}$$

a relation that may be recast in the following form for the field quadratures:

$$\begin{bmatrix}X_+(0,t)\\Y_+(0,t)\end{bmatrix}=\tilde{r}\begin{bmatrix}-\cos\phi & -\sin\phi\\ \sin\phi & -\cos\phi\end{bmatrix}\begin{bmatrix}X_-(0,t)\\Y_-(0,t)\end{bmatrix}+\tilde{t}\begin{bmatrix}X_+^{\rm vac}(0,t)\\Y_+^{\rm vac}(0,t)\end{bmatrix}\ , \tag{4.2b}$$

where $X_+^{\rm vac}$ and $Y_+^{\rm vac}$ are quadratures of the vacuum field defined via relations (3.12). Using Eqs. (3.14) to describe the effect of the nonlinear medium and Eqs. (4.1b) and (4.2b), the mirrors, one can now propagate the quadratures an entire round trip through the cavity with the result

$$\begin{bmatrix}X_+(0,t)\\Y_+(0,t)\end{bmatrix}=\tilde{r}\begin{bmatrix}\cos^2\phi+\sin^2\phi e^{2ql} & \cos\phi\sin\phi(1-e^{-2ql})\\ \cos\phi\sin\phi(e^{2ql}-1) & \cos^2\phi+\sin^2\phi e^{-2ql}\end{bmatrix}\times\begin{bmatrix}X_+(0,t-2l/c)\\Y_+(0,t-2l/c)\end{bmatrix}+\tilde{t}\begin{bmatrix}X_+^{\rm vac}(0,t)\\Y_+^{\rm vac}(0,t)\end{bmatrix}\ . \tag{4.3}$$

A suitable similarity transformation may now be performed so as to diagonalize the 2×2 evolution matrix in the preceding equation. Because of phase-sensitive amplification, characterized by different reference phases ϕ_+ and ϕ_- on the two halves of each round trip, the evolution matrix is not normal. Therefore, this similarity transformation is not a simple orthogonal rotation matrix and gives rise to linear combinations of the quadratures that are not orthogonal on the phasor diagram. Nevertheless, such a transformation is valuable since it determines those linear combinations of the quadratures that do not mix from one round trip to the next. As shown in Appendix B, a whole class of transformation matrices T

of the following form accomplishes this diagonalization:

$$T=\begin{bmatrix}\gamma_-(e^{-f}+e^{ql}\sin\phi) & \gamma_- e^{-ql}\cos\phi \\ \gamma_+ e^{ql}\cos\phi & -\gamma_+(e^{f}+e^{-ql}\sin\phi)\end{bmatrix}, \tag{4.4}$$

where f is determined through the relationship

$$\sinh f \equiv \sin\phi \sinh ql \ , \tag{4.5}$$

and the constants $\gamma_\pm$ are so far arbitrary. We wish, however, to be able to interpret the resulting linear combinations of quadratures as quadratures, albeit relative to different phase angles, say ϕ'_+ and ϕ'_- (with the two not differing by $\pi/2$, in general). To do so, we must pick $\gamma_\pm$ so that the sum of the squares of the elements in each row of T equals unity, i.e.,

$$\gamma_\pm=(e^{\mp 2f}+e^{\pm 2ql}+2e^{\mp(f-ql)}\sin\phi)^{-1/2} \ . \tag{4.6}$$

Under this transformation Eq. (4.3) becomes

$$\begin{bmatrix}X_+^T(-,t)\\ Y_+^T(0,t)\end{bmatrix}=\tilde{r}\begin{bmatrix}e^{2f} & 0\\ 0 & e^{-2f}\end{bmatrix}\begin{bmatrix}X_+^T(0,t-2l/c)\\ Y_+^T(0,t-2l/c)\end{bmatrix}+\tilde{t}\begin{bmatrix}X_+^{\mathrm{vac},T}(0,t)\\ Y_+^{\mathrm{vac},T}(0,t)\end{bmatrix} . \tag{4.7}$$

Threshold is obtained when the gain X_+^T experiences as it passes through the medium in time $2l/c$ compensates exactly for the loss at the output mirror. The nominal threshold condition is then given by

$$\tilde{r}e^{2f}=1 \ . \tag{4.8}$$

Note from this relation that $2f$ serves as an effective gain parameter of the parametric medium, which depends not only on the pump amplitude but also on the pump phase ϕ via Eq. (4.5).

We note from Eq. (4.5) that for $\phi=0$, for which $\phi_+=\phi_-$, the effective gain vanishes. This may be seen directly from Eqs. (3.14), from which one may show that the round-trip amplification of any quadrature of the intracavity field vanishes for $\phi=0$—the gain on one half of the trip is exactly negated by the attenuation on the other half. On the other hand, for $\phi=\pi/2$ the effective round-trip gain is at its largest. This modulation of gain with the relative phase between two nonlinearly coupled waves was first demonstrated by Wu and Kimble [15] in second-harmonic generation within an optical cavity. For $\phi=0$, the cavity resonance condition (nodes at the perfect mirror for both the pump wave and the subharmonic signal wave) is incompatible with the fact that the pump wave must be $\pi/2$ phase shifted relative to the signal wave that the former generates.

From Eq. (4.7) and the easily determined variance of any vacuum-field quadrature, one may calculate the steady-state variance of an arbitrary quadrature of the rightward-traveling field at $z=0$. Of most interest is the quadrature that exhibits minimum noise and thus governs the maximum squeezing possible in the parametric oscillator. We construct an arbitrary quadrature $Q_+(u,v)$ of the rightward-traveling field at the output mirror from a linear combination of X_+^T and Y_+^T as

$$Q_+(u,v)=uX_+^T(z=0)+vY_+^T(z=0) \ , \tag{4.9}$$

where the coefficients u and v are to be constrained by the relation

$$u^2+v^2+2uv\cos\delta\theta=1 \ , \tag{4.10}$$

which is the equation of an ellipse in the (u,v) plane. Here $\delta\theta$ is the difference of phases of the two nonorthogonal quadratures X_+^T and Y_+^T, which may be determined by taking the scalar product of the two rows of the matrix T [with normalizations (4.6)]:

$$\cos\delta\theta=T_{11}T_{21}+T_{12}T_{22} \ . \tag{4.11a}$$

It is shown in the second half of Appendix B that $\cos\delta\theta$ can be written in a simple form involving only f and ϕ:

$$\cos\delta\theta=\frac{\sinh f\cos\phi}{(\sinh^2 f+\sin^2\phi)^{1/2}} \ . \tag{4.11b}$$

The variance of $Q_+(u,v)$ involves the variances of X_+^T and Y_+^T and their covariances, which may be evaluated from Eq. (4.7) by noting that in the steady state all variances and covariances remain unchanged from one round trip to the next. Since the vacuum field is perfectly isotropic, they may all be expressed in terms of the variance of any quadrature of the vacuum field, say $\langle\Delta X_+^{\mathrm{vac}}(z=0)^2\rangle$, which we denote by N for brevity. Thus, for example,

$$\langle\Delta X_+^T(z=0)^2\rangle=\tilde{r}^2e^{4f}\langle\Delta X_+^T(z=0)^2\rangle+\tilde{t}^2\langle\Delta X_+^{\mathrm{vac},T}(z=0)^2\rangle \ ,$$

so that

$$\langle\Delta X_+^T(z=0)^2\rangle=\frac{(1-\tilde{r}^2)}{(1-\tilde{r}^2e^{4f})}N \ . \tag{4.12a}$$

Similarly,

$$\langle\Delta Y_+^T(z=0)^2\rangle=\frac{(1-\tilde{r}^2)}{(1-\tilde{r}^2e^{-4f})}N \tag{4.12b}$$

and

$$\langle\Delta X_+^T(z=0)\Delta Y_+^T(z=0)\rangle=\langle\Delta Y_+^T(z=0)\Delta X_+^T(z=0)\rangle^*=e^{-i\delta\theta}N \ . \tag{4.12c}$$

In arriving at Eq. (4.12c), we made use of the fact that

$$\langle\Delta X_+^{\mathrm{vac},T}(z=0)\Delta Y_+^{\mathrm{vac},T}(z=0)\rangle=e^{-i\delta\theta}\langle\Delta X_+^{\mathrm{vac},T}(z=0)^2\rangle=e^{-i\delta\theta}N \ .$$

From Eqs. (4.9) and (4.12), it now follows that

$$\langle\Delta Q_+(u,v)^2\rangle=N\left[\frac{(1-\tilde{r}^2)u^2}{1-\tilde{r}^2e^{4f}}+\frac{(1-\tilde{r}^2)v^2}{1-\tilde{r}^2e^{-4f}}+2uv\cos\delta\theta\right] , \tag{4.13}$$

where u and v are constrained by Eq. (4.10).

Although Eq. (4.13) describes the general situation, the quadrature of most interest, as we have indicated earlier,

is one that exhibits maximum squeezing, or equivalently minimum fluctuations. We thus wish to minimize the right-hand side of Eq. (4.13) in the (u,v) phase subject to the constraint (4.10). It is worth noting that the case of $\phi=\pi/2$ is special, since for this case $\cos\delta\theta$ is 0 and the minimization problem is rather trivial. The minimum variance is obtained for the Y quadrature, corresponding to $u=0$, $v=1$, and is given by Eq. (4.12b). The general optimization problem for arbitrary ϕ is, however, more involved and has been considered in detail in Appendix C.

The results are displayed in graphical form in Figs. 2–4. In Fig. 2, we consider the threshold parameter defined as $\chi\equiv\bar{r}\,e^{2f}$ to have a fixed value between 0 and 1 as the mirror reflectance $\bar{r}$ is varied. Since the effective gain parameter f is non-negative, the largest value of $\bar{r}$ allowed for a given value of χ is χ itself, for which the active-medium gain f is 0. We see from these curves that in each case the quantum noise in the quietest quadrature of the intracavity field first decreases from the vacuum level as $\bar{r}$ increases from 0 (limit of no cavity) until some lowest value is attained. Then as $\bar{r}$ approaches χ (or equivalently, f approaches 0), the noise level begins to rise to the vacuum level. This behavior of the curves is a result of competition between two effects: A larger $\bar{r}$ allows a larger effective interaction time for the field and the nonlinear medium, but, at the same time, since χ is fixed, a smaller effective gain parameter f that controls the single-round-trip squeezing. Of the three curves on this figure, the one for which χ is closest to 1 has the best overall noise reduction as a function of the mirror reflectance.

In Fig, 3, the value of the effective gain parameter f is treated as being fixed for each curve. As the value of $\bar{r}$ ranges from 0 (no cavity) to e^{-2f} (threshold), the quantum noise in the quietest quadrature of the rightward-traveling cavity field at the output mirror decreases from the vacuum level to 50% of the vacuum level. Of the three curves, the one for which the gain parameter f is the largest shows, as expected, the best overall noise reduction or squeezing as a function of the mirror reflectance. The curves terminate at $\bar{r}=e^{-2f}$ where the minimum variance assumes the threshold value calculated later in Eq. (4.14).

In Fig. 4, we have studied the dependence of squeezing of the cavity field on the phase ϕ of the pump. In this figure, the value of the pump amplitude and therefore ql is maintained fixed at $\exp(ql)=1.2$, as the pump phase varies from 30° to 75°. As ϕ increases, so does the effective pump parameter f [see Eq. (4.5)] and so the squeezing is enhanced, as is clearly evident from the figure. In other words, the best overall squeezing is expected for $\phi=90°$. The end points of the curves refer to the threshold squeezing given by Eq. (4.14).

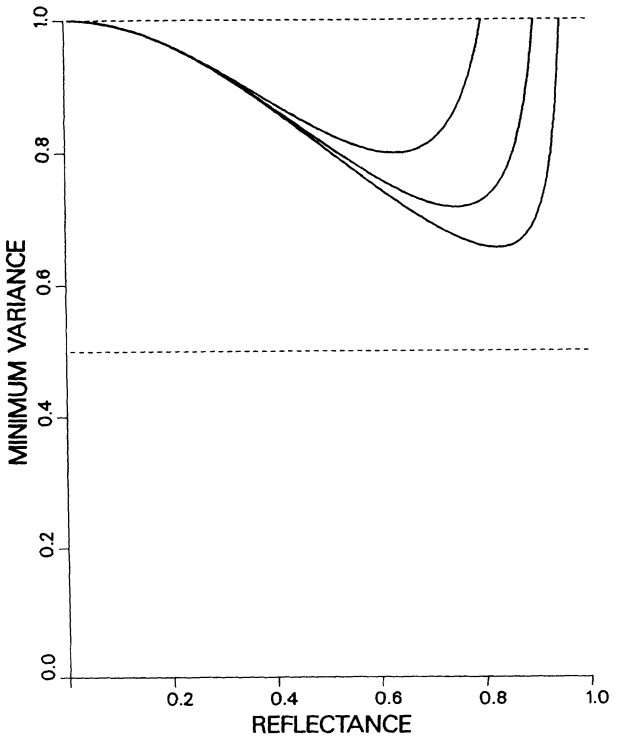

FIG. 2. Variance of the quietest quadrature, normalized by dividing by N, of the right-traveling piece of the intracavity field at the output mirror, $z=0$, vs output-mirror reflectance $\bar{r}$, for fixed pump phase $\phi=45°$ and threshold parameter χ. The three curves from left to right on the figure have χ values 0.8, 0.9, and 0.95, respectively.

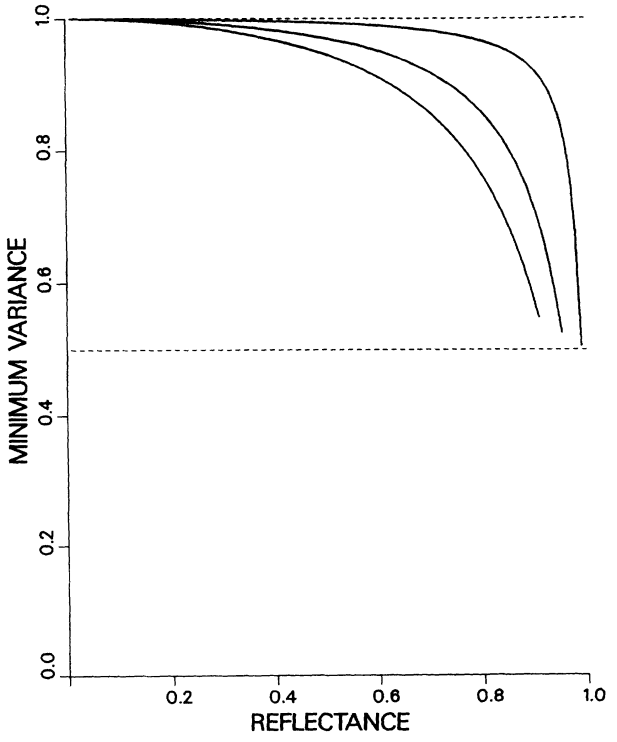

FIG. 3. Variance of the quietest quadrature, normalized by dividing by N, of the right-traveling piece of the intracavity field at the output mirror, $z=0$, vs output-mirror reflectance $\bar{r}$, for fixed pump phase $\phi=45°$ and effective gain parameter f. The three curves from left to right on the figure have $\exp(2f)$ equal to 1.10, 1.05, and 1.01, respectively.

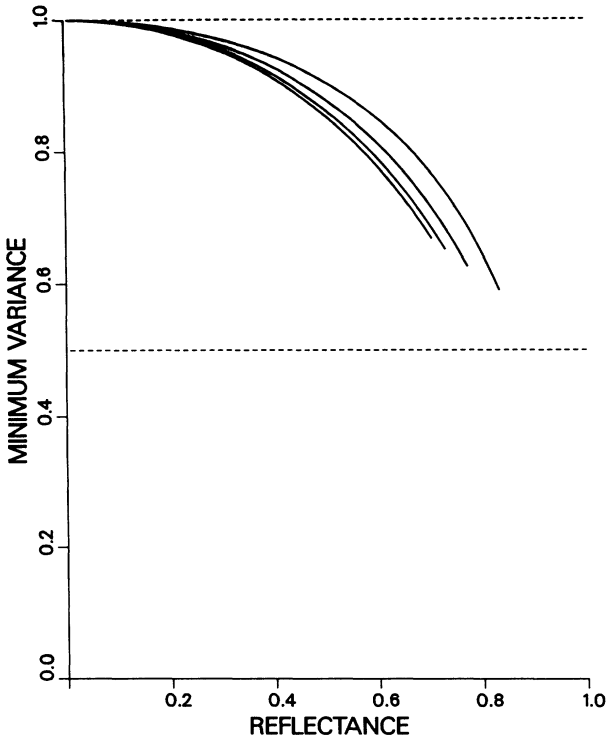

FIG. 4. Variance of the quietest quadrature, normalized by dividing by N, of the right-traveling piece of the intracavity field at the output mirror, $z=0$, vs output-mirror reflectance $\bar{r}$ for fixed pump amplitude: $\exp(ql)=1.2$. The four curves from left to right on the figure have pump phase ϕ equal to 75°, 60°, 45°, and 30°, respectively.

Squeezing just below threshold: $\bar{r}e^{2f}\rightarrow 1$

There is one special case for which the maximum squeezing is fairly simple to calculate exactly. This is the case of the parametric oscillator just below threshold, $\bar{r}e^{2f}\rightarrow 1$. As we note quickly from Eq. (4.13), in this limit the coefficient of the u^2 term becomes infinite, and so the minimum variance for the quadrature $Q(u,v)$ of the rightward-traveling intracavity field at $z=0$ is obtained when $u^2=0$ and $v^2=1$. In other words, the Y_+^T quadrature shows minimum fluctuations at threshold, and from Eqs. (4.13) it follows that the maximum degree of squeezing is merely

$$\chi_S=1-\frac{1-\bar{r}^2}{1-\bar{r}^2}=\frac{\bar{r}^2}{1+\bar{r}^2}\ . \tag{4.14}$$

This expression tends to the correct value [2,4] of $\frac{1}{2}$, or 50%, in the good-cavity limit, $\bar{r}\rightarrow 1$, and 0 in the opposite limit of 100% output coupling.

For the general situation below threshold, it is worth noting from the last result of Appendix C that the minimum variance is in general smaller than

$$N\frac{1-\bar{r}^2}{1-\bar{r}^2e^{-4f}}\ ,$$

which is the variance of the Y_+^T quadrature of the intracavity field. Only when either $\cos\delta\theta$ or $\sin\delta\theta$ is 0 or at threshold, as we have just seen, is the minimum variance exactly equal to the variance of the Y_+^T quadrature.

V. SPECTRUM OF FLUCTUATIONS OF THE OUTPUT FIELD

Outside the cavity ($z<0$), the quasimode structure described by the M_k's no longer exists. Without these quasimodes one may wish to consider examining the squeezing of the individual universe modes. However, as Gea-Banacloche *et al.* [6] have noted, this would require an integration of the output field over a time longer than $2L/c$, but such long times would cause unphysical effects having to do with reflections from the auxiliary mirror at $z=-L$.

To circumvent this problem, the authors introduced a finite Fourier transform in which the time of integration T_m is less than $2L/c$ but large compared to $2l/c$, so that a high frequency precision of order $2\pi/T_m$ can be attained in the spectral analysis of the fluctuations of the output field. The transform at frequency offset $\delta\omega$ from the resonance is then a superposition of several universe modes centered at that offset frequency in a bandwidth $2\pi/T_m$,

$$\hat{e}^{\,\mathrm{out}}(\delta\omega)=\frac{\mathcal{N}}{(T_m)^{1/2}}\int_0^{T_m}e^{\mathrm{out}}(t)e^{i\delta\omega t}dt\ , \tag{5.1}$$

where $\mathcal{N}$ is a normalization constant chosen so that

$$[\hat{e}^{\,\mathrm{out}}(\delta\omega),\hat{e}^{\,\mathrm{out}}(\delta\omega)^{\dagger}]=1\ . \tag{5.2}$$

With this choice of the normalization, $\hat{e}^{\,\mathrm{out}}(\delta\omega)$ may be interpreted as a single-mode annihilation operator. Exactly the same considerations as these apply to the incoming vacuum field $e^{\mathrm{vac}}(0,t)$ as well.

The outgoing field $e^{\mathrm{out}}(t)$ arises from the transmitted left-traveling wave inside the cavity and also includes a contribution from the vacuum partially reflected off the output mirror,

$$e^{\mathrm{out}}(t)=\tilde{t}e_-(0,t)+\bar{r}e^{\mathrm{vac}}(0,t)\ . \tag{5.3a}$$

By using Eq. (4.2a), we may rewrite this relation in terms of the e_+ field as

$$e^{\mathrm{out}}(t)=-\frac{\tilde{t}}{\bar{r}}e_+(0,t)+\frac{1}{\bar{r}}e^{\mathrm{vac}}(0,t)\ . \tag{5.3b}$$

Since $\bar{r}$ and $\tilde{t}$ are both real, this relation also holds for any quadrature of these fields as well, both in time and frequency domains. Thus, for example, in the frequency domain,

$$\begin{bmatrix}\hat{X}_+^{\mathrm{out},T}(\delta\omega)\\ \hat{Y}_+^{\mathrm{out},T}(\delta\omega)\end{bmatrix}=-\frac{\tilde{t}}{\bar{r}}\begin{bmatrix}\hat{X}_+^{T}(0,\delta\omega)\\ \hat{Y}_+^{T}(0,\delta\omega)\end{bmatrix}+\frac{1}{\bar{r}}\begin{bmatrix}\hat{X}_+^{\mathrm{vac},T}(0,\delta\omega)\\ \hat{Y}_+^{\mathrm{vac},T}(0,\delta\omega)\end{bmatrix}\ . \tag{5.4}$$

The superscript T denotes the same transformation as performed in the previous section. Note that the Fourier transform of a quadrature field like $X_+^{\mathrm{out},T}(t)$ produces a generalized quadrature [16,17,6] in the frequency do-

main, involving a pair of frequencies $\delta\omega$ and $-\delta\omega$ of the original field $e^{\text{out}}(t)$.

The quadratures of the $e_+(0,t)$ field that occur on the right-hand side of the preceding equation in the frequency domain may be obtained easily in terms of the vacuum-field quadratures by Fourier transforming [via Eq. (5.1)] the relation (4.7). Since in the large-T_m limit, the Fourier transform of any function $f(t)$ and its time-displaced form $f(t-\tau)$ differ merely by a multiplicative factor $e^{i\delta\omega\tau}$, it follows that

$$\begin{bmatrix} \hat{X}_+^T(0,\delta\omega) \\ \hat{Y}_+^T(0,\delta\omega) \end{bmatrix} = \tilde{t} \begin{bmatrix} (1-\tilde{r}e^{2f}e^{i\delta\omega 2l/c})^{-1} & 0 \\ 0 & (1-\tilde{r}e^{-2f}e^{i\delta\omega 2l/c})^{-1} \end{bmatrix} \begin{bmatrix} \hat{X}_+^{\text{vac},T}(0,\delta\omega) \\ \hat{Y}_+^{\text{vac},T}(0,\delta\omega) \end{bmatrix} . \tag{5.5}$$

It is now only a matter of a simple substitution of this relation in Eq. (5.4) and the use of the identity $1-\tilde{t}^2=\tilde{r}^2$ to show the following connection between the output field and the vacuum field in the frequency domain:

$$\begin{bmatrix} \hat{X}_+^{\text{out},T}(\delta\omega) \\ \hat{Y}_+^{\text{out},T}(\delta\omega) \end{bmatrix} = \begin{bmatrix} \dfrac{\tilde{r}-e^{2f}e^{i\delta\omega 2l/c}}{1-\tilde{r}e^{2f}e^{i\delta\omega 2l/c}} & 0 \\ 0 & \dfrac{\tilde{r}-e^{-2f}e^{i\delta\omega 2l/c}}{1-\tilde{r}e^{-2f}e^{i\delta\omega 2l/c}} \end{bmatrix} \begin{bmatrix} \hat{X}_+^{\text{vac},T}(0,\delta\omega) \\ \hat{Y}_+^{\text{vac},T}(0,\delta\omega) \end{bmatrix} . \tag{5.6}$$

The preceding equation enables one to determine the spectrum [5] of quantum noise, or equivalently, squeezing, for the output field. In what follows, we shall restrict our attention to the case of zero detuning, $\delta\omega=0$, since we expect to see maximum squeezing for this special situation and also since the general case of nonzero detuning can be handled very similarly [6]. For $\delta\omega=0$, all quadratures such as $\hat{X}_+^{\text{out},T}$ are Hermitian and their variances and covariances are, from Eq. (5.6), the following:

$$\langle \Delta\hat{X}_+^{\text{out},T}(0)^2\rangle = \left[\frac{\tilde{r}-e^{2f}}{1-\tilde{r}e^{2f}}\right]^2 N' , \tag{5.7a}$$

$$\langle \Delta\hat{Y}_+^{\text{out},T}(0)^2\rangle = \left[\frac{\tilde{r}-e^{-2f}}{1-\tilde{r}e^{-2f}}\right]^2 N' ,$$

and

$$\langle \Delta\hat{X}_+^{\text{out},T}(0)\Delta\hat{Y}_+^{\text{out},T}(0)\rangle = \langle \Delta\hat{Y}_+^{\text{out},T}(0)\Delta\hat{X}_+^{\text{out},T}(0)\rangle^* = e^{-i\delta\theta}N' , \tag{5.7b}$$

where N' denotes the variance of any quadrature of the vacuum field, say $\langle \Delta\hat{X}_+^{\text{vac},T}(0)^2\rangle$, and $\delta\theta$, the difference between the phase angles of the transformed X and Y quadratures, can be computed as before via Eq. (4.11).

Armed with these variances and covariances, we may now write down the variance of the central Fourier component of an arbitrary quadrature of the output field. We follow the same procedure as in the preceding section to determine that quadrature that has the smallest variance. The results of Appendix C are again applicable, albeit with different values for parameters a and b. It is worth noting that since a and b here assume values that are different from those for the intracavity field, the quadrature that has minimum fluctuations in the intracavity field is in general not the one that displays minimum fluctuations in the output field and vice versa.

The results are shown in graphical form in Figs. 5–7. In Fig. 5, we fix the value of threshold parameter χ, which is less than 1, while the reflectance $\tilde{r}$ is varied from 0 to 1. It is evident that for all values of χ, the squeezing of the central Fourier component of the output field is nearly perfect at very high output-mirror coupling (low

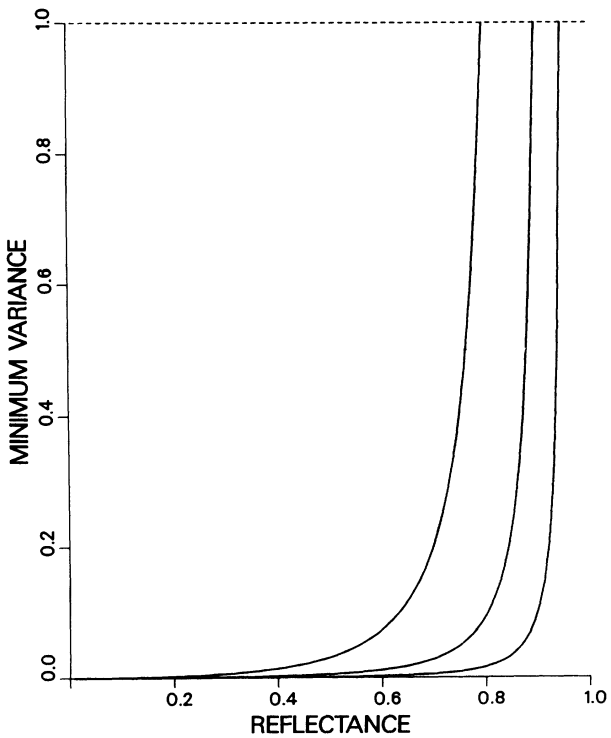

FIG. 5. Variance of the central Fourier frequency component ($\delta\omega=0$) of the quietest quadrature, normalized by dividing by N', of the output field at the output mirror, $z=0$, vs output-mirror reflectance $\tilde{r}$, for fixed pump phase $\phi=45°$ and threshold parameter χ. The three curves from left to right on the figure have χ values 0.8, 0.9, and 0.95, respectively.

$\bar{r}$), degrading as the cavity becomes less and less transmitting. This behavior can be understood in the following way. Since χ is held constant, a low value of $\bar{r}$ implies a large effective gain or squeezing parameter f as well as only a small contamination of the output field by incoming vacuum light reflected into the output field by the output mirror [see Eq. (5.3a)]. Thus the output light results mainly from the incoming transmitted vacuum field, which undergoes large squeezing as it circulates through the high-gain parametric medium. As the output coupling decreases, the gain parameter of the parametric medium decreases as well, if χ is held fixed, and the contamination of the output by the reflected incoming vacuum field increases. Therefore, in the limit of low output coupling the squeezing of the output field decreases for fixed χ.

In Fig. 6, on the other hand, the value of the gain parameter f is held fixed. Clearly, for this case, as the output mirror becomes less and less transmitting, the squeezing of field fluctuations by the parametric amplification process happens over an ever-increasing number of round trips. Thus, the degree of squeezing both of the cavity and output fields is enhanced as $\bar{r}$ rises to 1. Furthermore, since the leftmost curve on this figure has the largest value of f of the three curves, it represents the largest overall squeezing.

In Fig. 7, we display the dependence of squeezing of

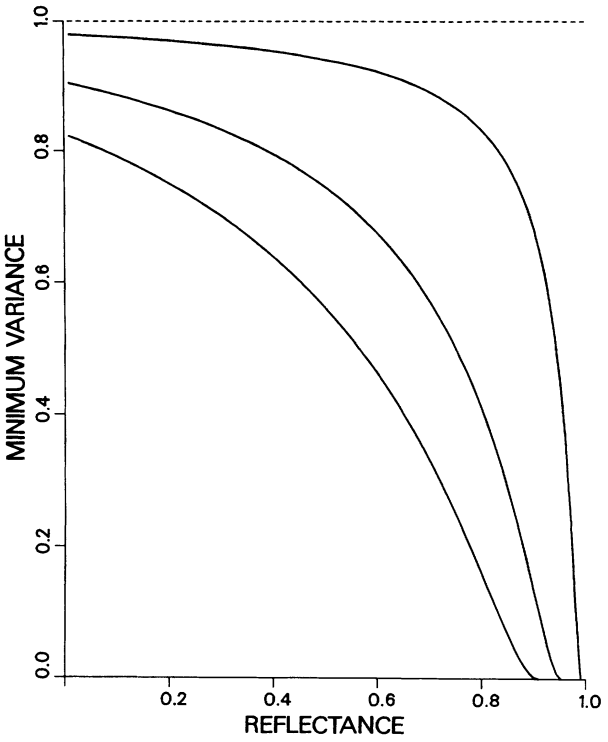

FIG. 6. Variance of the central Fourier frequency component ($\delta\omega=0$) of the quietest quadrature, normalized by dividing by N', of the output field at the output mirror, $z=0$, vs output-mirror reflectance $\bar{r}$, for fixed pump phase $\phi=45°$ and effective gain parameter f. The three curves from left to right on the figure have $\exp(2f)$ equal to 1.10, 1.05, and 1.01, respectively.

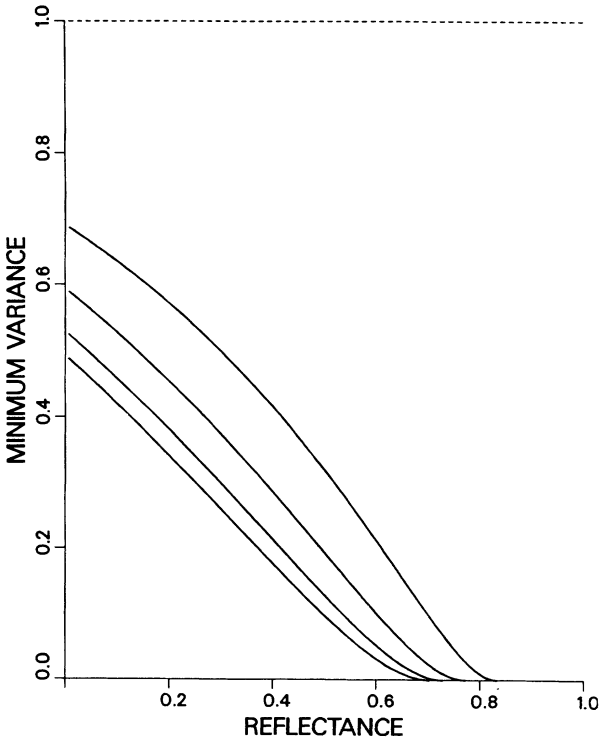

FIG. 7. Variance of the central Fourier frequency component ($\delta\omega=0$) of the quietest quadrature, normalized by dividing by N', of the output field at the output mirror, $z=0$, vs output-mirror reflectance $\bar{r}$ for fixed pump amplitude: $\exp(ql)=1.2$. The four curves from left to right on the figure have pump phase ϕ equal to 75°, 60°, 45°, and 30°, respectively.

the central frequency component of the output field on reflectance for a fixed value of the pump amplitude, or equivalently of the parameter ql, while the value of the pump phase ϕ is changed from curve to curve. We set $\exp ql=1.2$, while the value of ϕ changes from 30° to 75°, as in Fig. 4. Once again for the same reason as in Fig. 4, namely that as ϕ increases, so does the effective gain parameter f, we have enhanced squeezing with increasing phase angle. As in the preceding section, we now consider explicitly the situation just below threshold, i.e., as $\bar{r}e^{2f}\rightarrow 1$.

Squeezing just below threshold: $\bar{r}e^{2f}\rightarrow 1$

Since at threshold the variance of the X_+^T quadrature becomes infinite [Eq. (5.7a)], it is evident that any admixture, however small, of this quadrature in the construction of a general quadrature will give rise to an infinite value for the variance of the latter. In other words, the minimum variance is obtained only for the Y_+^T quadrature of the output field. Furthermore, it follows from Eq. (5.7a) that this minimum variance vanishes at threshold, regardless of the degree of output-mirror coupling $\bar{t}^2$. (In Fig. 5, for example, this situation would be represented by a line that coincides with the abscissa for $\bar{r}\neq 1$ with a step discontinuity of 1 at $\bar{r}=1$). Thus, the Y_+^T quadrature of the central frequency component of the output

field is perfectly squeezed just below threshold, while any other quadrature of this field has infinite variance.

There is one other conclusion worthy of note here. Even if $\bar{r}=0$, which amounts to a perfectly transmitting output mirror, the Y_+^T quadrature of the output field still exhibits some squeezing, namely that its variance is lower than that of the vacuum field by a factor of e^{-4f}. This is a result of the fact that although the output mirror is fully transmitting, the output field from the cavity arises from the vacuum field entering the cavity at $z=0$ and then amplifying (and getting squeezed) through a round trip before emerging at $z=0$.

VI. CONCLUSIONS AND OUTLOOK

We have considered in this paper the fully quantum-mechanical problem of a degenerate parametric oscillator operating below threshold. The main objective of this work has been to develop a theory of matter-field interaction inside a cavity with arbitrary output-mirror coupling and to illustrate this theory for the optical parametric oscillator.

There are at least four aspects of the problem that need further attention. The first concerns the somewhat *ad hoc* nature of the effective-Hamiltonian approach adopted in the present work. This phenomenological approach cannot satisfactorily incorporate the effect of spontaneous emission and must be supplanted by a fully microscopic theory of nonlinear parametric interaction. Clearly spontaneous-emission noise will compromise the maximum squeezing available in a parametric oscillator or any other nonlinear active device.

A relatively straightforward extension of this work concerns a double-sided cavity, one that allows light to emerge from both sides of the cavity. This extension must be considered if one is to treat the problem of coupling of several parametric oscillators in series.

A third important extension of the present work is an analysis of the above-threshold behavior of the parametric oscillator. Here one needs to address the question of saturation of both the pump and signal intensities either via an effective Hamiltonian or by developing a fully microscopic theory. As we have noted earlier, a microscopic approach will have the added advantage of lending itself well to a natural and correct inclusion of spontaneous-emission noise.

The question of pump amplitude and phase noise is also an important one, particularly if one is to apply the present theory to realistic experiments. It would seem that a purely classical theory of noise may suffice here. However, squeezing of the pump noise, which can only be treated quantum mechanically, may also be an interesting problem to consider, since the noise reduction of the signal field will depend critically upon such squeezing.

APPENDIX A: THE FUNCTIONS $G_\pm(z,z')$

We first note from Eq. (3.8) that

$$G_+(z,z')=-G_-^*(z,z') .$$

So we need only consider one of the two functions, say $G_+(z,z')$. We first rewrite $G_+(z,z')$ by splitting $\sin[k(z'-l)]$ into its exponentials:

$$G_+(z,z')=-\frac{\hbar\Omega_0}{4c\epsilon_0 AL}\sum_k M_k^2(e^{ik(z'-l)}-e^{-ik(z'-l)}) \times e^{i\delta\Omega_k z/c}e^{-ikl} . \tag{A1}$$

In terms of the detuning $\delta\Omega_k=c(k-k_0)$, we may recast the above equation in the form

$$G_+(z,z')=-\frac{\hbar\Omega_0}{4c\epsilon_0 AL}\left[e^{ik_0(z'-2l)}\sum_k M_k^2 e^{i\delta\Omega_k(z+z'-2l)/c} -e^{-ik_0 z'}\sum_k M_k^2 e^{i\delta\Omega_k(z-z')/c}\right] . \tag{A2}$$

From the periodic nature of M_k^2 as a function of k and from the shift property of the exponential function

$$e^{az}\rightarrow e^{as}e^{az} \text{ under } z\rightarrow z+s ,$$

it follows that each of the finite k sums in Eq. (A1) may be reduced to a finite k sum over a single period of M_k^2 of length π/l. Picking this period to be the one centered at k_0, we may rewrite Eq. (A2) as

$$G_+(z,z')=-\frac{\hbar\Omega_0}{4c\epsilon_0 AL}\left[e^{ik_0(z'-2l)}\sum_k{}' M_k^2 e^{i\delta\Omega_k(z+z'-2l)/c}\sum_{n=-\infty}^{\infty} e^{in\pi(z+z'-2l)/l} -e^{-ik_0 z'}\sum_k{}' M_k^2 e^{i\delta\Omega_k(z-z')/c}\sum_{n=-\infty}^{\infty} e^{in\pi(z-z')/l}\right] , \tag{A3}$$

in which the prime on the summation sign represents a restricted k sum over the fundamental period $[k_0-\pi/2l, k_0+\pi/2l]$.

We now use the identity

$$\sum_{n=-\infty}^{\infty} e^{in\pi x/l}=2l\sum_{m=-\infty}^{\infty}\delta(x-2ml)$$

in Eq. (A3). By noting the fact that for the physical situ-

ation at hand, $0<z,z'<l$, we see that in Eq. (A3) the first resulting δ-function sum will have no contributing terms, while in the second such sum only the term $\delta(z-z')$ will contribute. The net result of this observation is that Eq. (A3) reduces to the following simple form:

$$G_+(z,z')=\frac{\hbar\Omega_0 l}{2c\epsilon_0 AL}e^{-ik_0 z}\delta(z-z')\sum_k{}' M_k^2 . \tag{A4}$$

One may carry out the k sum above by recalling that in the limit $L\to\infty$, the universe modes become continuous in k with a density of modes L/π, so that

$$\begin{aligned}\sum_k{}' M_k^2&=\frac{L}{\pi}\int_{-\pi/2l}^{\pi/2l}M_k^2\\&=\frac{2Lp}{\pi l}\int_0^{\pi/2}d\theta\frac{1}{\sin^2\theta+p^2\cos^2\theta}\\&=\frac{L}{l},\end{aligned}$$

in which use was made of expression (2.2) for M_k and the known integral identity

$$\int_0^{\pi/2}d\theta\frac{1}{\sin^2\theta+p^2\cos^2\theta}=\frac{\pi}{2p} .$$

With this simplification, Eq. (A4) may be reexpressed in its final form as

$$G_+(z,z')=\frac{\hbar\Omega_0}{2c\epsilon_0 A}e^{-ik_0 z}\delta(z-z') . \tag{A5}$$

APPENDIX B: THE SIMILARITY TRANSFORMATION T

We seek here a similarity transformation matrix T that will diagonalize the following evolution matrix M:

$$M=\begin{bmatrix}\cos^2\phi+\sin^2\phi e^{2ql} & \cos\phi\sin\phi(1-e^{-2ql})\\ \cos\phi\sin\phi(e^{2ql}-1) & \cos^2\phi+\sin^2\phi e^{-2ql}\end{bmatrix} . \tag{B1}$$

In other words, we wish to find the class of matrices T such that

$$TMT^{-1}=M_\Delta , \tag{B2}$$

in which M_Δ is diagonal.

Since a similarity transformation leaves the eigenvalues of a matrix invariant, it is clear that the eigenvalues of M are the diagonal elements of M_Δ. Furthermore, since Eq. (B2) may be rewritten as

$$MT^{-1}=T^{-1}M_\Delta ,$$

it follows that the eigenvectors of M form the columns of the matrix T^{-1} whose inverse T is the matrix we seek. Evidently, then, the problem of finding T reduces to the problem of finding the eigenvalues and eigenvectors of M.

1. Eigenvalues and eigenvectors of M

The eigenvalues λ obey the following quadrature equation:

$$\begin{aligned}&(\cos^2\phi+\sin^2\phi e^{2ql}-\lambda)(\cos^2\phi+\sin^2\phi e^{-2ql}-\lambda)\\&\qquad=\cos^2\phi\sin^2\phi(1-e^{-2ql})(e^{2ql}-1) .\end{aligned}$$

This may be expanded into the following equation:

$$\lambda^2-2\lambda(\cos^2\phi+\sin^2\phi\cosh 2ql)+[\cos^4\phi+\sin^4\phi+2\cos^2\phi\sin^2\phi(\cosh 2ql-2\sinh^2 ql)]=0 .$$

Using the identities $\cosh 2ql=2\sinh^2 ql+1$ and $\sin^2\phi+\cos^2\phi=1$, we reduce this equation to the form

$$\lambda^2-2\lambda(1+2\sin^2\phi\sinh^2 ql)+1=0 .$$

By now introducing a symbol f by the relation

$$\sinh f\equiv\sin\phi\sinh ql , \tag{B3}$$

it is easy to show that the above quadratic equation reduces further to

$$\lambda^2-2\lambda\cosh 2f+1=0 ,$$

whose roots are simply

$$\lambda_\pm=e^{\pm 2f} . \tag{B4}$$

If $x_\pm$ are the eigenvectors for $\lambda_\pm$,

$$x_\pm=\begin{bmatrix}u_\pm\\ v_\pm\end{bmatrix} ,$$

then the ratios $u_\pm/v_\pm$ may be determined by either of the two relations

$$\frac{u_\pm}{v_\pm}=-\frac{M_{12}}{M_{11}-\lambda_\pm}=-\frac{M_{22}-\lambda_\pm}{M_{21}} , \tag{B5}$$

where M_{ij} denotes the ij matrix element of M. We pick the latter relation for computing u_+/v_+ and the former for u_-/v_-. Thus,

$$\begin{aligned}\frac{u_+}{v_+}&=-\frac{1-\sin^2\phi(1-e^{-2ql})-e^{2f}}{\sin\phi\cos\phi(e^{2ql}-1)}\\&=\frac{2e^f\sinh f+2\sin^2\phi\sinh ql e^{-ql}}{2\sin\phi\cos\phi\sinh ql e^{ql}}\\&=\frac{e^f+\sin\phi e^{-ql}}{\cos\phi e^{ql}} .\end{aligned} \tag{B6}$$

Note that we have made repeated use of Eq. (B3) in arriving at the above result. One may show in a similar way that the eigenvector corresponding to eigenvalue λ_- is given by

$$\frac{u_-}{v_-}=-\frac{\cos\phi e^{-ql}}{e^{-f}+\sin\phi e^{ql}} . \tag{B7}$$

Of course, each eigenvector is determined only up to an arbitrary normalization constant, which means that the matrix T^{-1} whose columns these eigenvectors constitute is determined only up to arbitrary normalization constants. Clearly, therefore, T too is arbitrary up to these normalization constants. In other words, there is a whole class of similarity transformations that will diagonalize M. Since

$$T^{-1}=\begin{bmatrix} u_+ & u_- \\ v_+ & v_- \end{bmatrix} ,$$

it follows that up to normalization factors the desired similarity transformation matrix T is

$$T=\begin{bmatrix} -v_- & u_- \\ v_+ & -u_+ \end{bmatrix} ,$$

with the ratios $u_\pm/v_\pm$ given by Eqs. (B6) and (B7).

2. Expressing $\cos\delta\theta$ in terms of f and ϕ

By noting from (B3) that $e^{f}+e^{-ql}\sin\phi=e^{-f}+e^{ql}\sin\phi$, we have from (4.4) and (4.11a) that

$$\cos\delta\theta=2\gamma_+\gamma_-(e^{-f}+e^{ql}\sin\phi)\sinh ql\cos\phi . \tag{B8}$$

Now one may show from Eq. (4.6) that when $1/\gamma_+^2$ and $1/\gamma_-^2$ are multiplied together, the nine terms obtained may be grouped as

$$1/\gamma_+^2\gamma_-^2=2+4\sin^2\phi+2\cosh(2f+2ql)+8\sin\phi\cosh(f+ql) .$$

This expression is further simplified by using the identity

$$\cosh 2(f+ql)=2\sinh^2(f+ql)-1$$

to the form

$$1/\gamma_+^2\gamma_-^2=4[\sin\phi+\cosh(f+ql)]^2 .$$

We now use the relation (B3) to write

$$\begin{aligned}\cosh(f+ql)&=\cosh f\cosh ql+\sinh f\sinh ql\\ &=\cosh f(1+\sinh^2 f/\sin^2\phi)^{1/2}+\sinh^2 f/\sin\phi\\ &=\frac{1}{\sin\phi}[\cosh f(\sinh^2 f+\sin^2\phi)^{1/2}+\sinh^2 f] ,\end{aligned}$$

and so from the previous equation it follows that

$$2\gamma_+\gamma_-=\frac{\sin\phi}{\sin^2\phi+\sinh^2 f+\cosh f(\sinh^2 f+\sin^2\phi)^{1/2}} . \tag{B9}$$

From Eq. (B3), one may solve for $e^{ql}\sin\phi$ by noting that

$$\begin{aligned}e^{ql}\sin\phi&=(\sinh ql+\cosh ql)\sin\phi\\ &=[\sinh f+(\sinh^2 f+\sin^2\phi)^{1/2}] .\end{aligned} \tag{B10}$$

By now observing that $e^{-f}+\sinh f=\cosh f$ and using Eqs. (B8), (B9), and (B10), one may see that

$$\cos\delta\theta=\frac{\sinh f\cos\phi}{(\sinh^2 f+\sin^2\phi)^{1/2}} ,$$

provided use is made of Eq. (B3) as well.

APPENDIX C: A CONSTRAINED MINIMIZATION PROBLEM

We wish here to provide the details of the minimization of the fluctuations (4.13), subject to the constraint (4.10). In simpler notation, the problem is to minimize

$$f(u,v)=au^2+bv^2+2cuv , \tag{C1}$$

subject to the constraint

$$u^2+v^2+2cuv=1 . \tag{C2}$$

We first note that by rotating the u-v axes by 45°, we transform Eq. (4.10) of the constraint ellipse to its "diagonal" form which does not have the "mixed" uv term. This diagonal form may be parametrized in terms of a single angle. Symbolically, if we let

$$u=\frac{1}{\sqrt{2}}(u'+v'),\quad v=\frac{1}{\sqrt{2}}(-u'+v') , \tag{C3}$$

then Eq. (C2) becomes

$$u'^2(1-c)+v'^2(1+c)=1 ,$$

which may be parametrized as

$$u'=\frac{1}{\sqrt{1-c}}\cos\theta,\quad v'=\frac{1}{\sqrt{1+c}}\sin\theta . \tag{C4}$$

In terms of the parametrization angle θ, the function $f(u,v)$ to be minimized may be recast as

$$\begin{aligned}F(\theta)=&\frac{a}{2}\left[\frac{\cos\theta}{\sqrt{1-c}}+\frac{\sin\theta}{\sqrt{1+c}}\right]^2\\ &+\frac{b}{2}\left[-\frac{\cos\theta}{\sqrt{1-c}}+\frac{\sin\theta}{\sqrt{1+c}}\right]^2\\ &+c\left[\frac{\sin^2\theta}{1+c}-\frac{\cos^2\theta}{1-c}\right] ,\end{aligned}$$

which is of form

$$F(\theta)=a'\cos^2\theta+b'\sin^2\theta+2c'\sin\theta\cos\theta , \tag{C5}$$

where

$$\begin{aligned}a'&\equiv\frac{a+b-2c}{2(1-c)} ,\\ b'&\equiv\frac{a+b+2c}{2(1+c)} ,\\ c'&\equiv\frac{a-b}{2\sqrt{1-c^2}} .\end{aligned} \tag{C6}$$

The solution of the minimization problem, which is now reduced to a form involving a single parameter θ, may be completed as follows. By using the trigonometric

identities

$$\cos^2\theta=\tfrac{1}{2}(1+\cos 2\theta)\ ,$$

$$\sin^2\theta=\tfrac{1}{2}(1-\cos 2\theta)\ ,$$

$$2\sin\theta\cos\theta=\sin 2\theta$$

and by defining another angle α by the relations

$$\cos\alpha=\frac{(a'-b')/2}{[(a'-b')^2/4+c'^2]^{1/2}}\ ,$$
$$\sin\alpha=\frac{c'}{[(a'-b')^2/4+c'^2]^{1/2}}\ , \tag{C7}$$

one may rewrite expression (C5) as

$$F(\theta)=\frac{a'+b'}{2}+[(a'-b')^2/4+c'^2]^{1/2}\cos(2\theta-\alpha)\ . \tag{C8}$$

Clearly, the minimum and maximum values of this expression are attained for $\theta=\alpha/2+\pi/2$ and $\theta=\alpha/2(\mathrm{mod}\pi)$, respectively, and they are

$$\min F(\theta)=\frac{a'+b'}{2}-[(a'-b')^2/4+c'^2]^{1/2}\ ,$$
$$\max F(\theta)=\frac{a'+b'}{2}+[(a'-b')^2/4+c'^2]^{1/2}\ . \tag{C9}$$

We may rewrite these expressions in terms of the original parameters a, b, and c by making use of the definitions (C6). After straightforward algebra, one may show that a useful final form in which the expressions in Eq. (C9) may be written is the following:

$$\min f(u,v)=\frac{a+b-2c^2}{2s^2}-\frac{1}{2s^2}\{[a-b-2c^2(1-b)]^2+4c^2s^2(1-b)^2\}^{1/2}\ ,$$
$$\max f(u,v)=\frac{a+b-2c^2}{2s^2}+\frac{1}{2s^2}\{[a-b-2c^2(1-b)]^2+4c^2s^2(1-b)^2\}^{1/2}\ , \tag{C10}$$

where $s^2=1-c^2$. Since in our problem c stands for $\cos\delta\theta$, s is merely a short form for $\sin\delta\theta$. A useful by-product of this form for $\min f(u,v)$ is that this minimum is in general smaller than

$$\frac{a+b-2c^2}{2s^2}-\frac{a-b-2c^2(1-b)}{2s^2}\ ,$$

or simply b.

[1] See, for example, D. Walls, Nature (London) **306**, 141 (1983); **324**, 210 (1986); R. Loudon and P. Knight, J. Mod. Opt. **34**, 709 (1987).
[2] G. Milburn and D. Walls, Opt. Commun. **39**, 401 (1981).
[3] B. Yurke, Phys. Rev. A **29**, 408 (1984).
[4] M. J. Collett and C. W. Gardiner, Phys. Rev. A **30**, 1386 (1984); C. W. Gardiner and M. J. Collett, *ibid.* **31**, 3761 (1985); C. W. Gardiner and C. M. Savage, Opt. Commun. **50**, 173 (1984).
[5] H. J. Carmichael, J. Opt. Soc. Am. B **4**, 1588 (1987).
[6] J. Gea-Banacloche, N. Lu, L. M. Pedrotti, S. Prasad, M. O. Scully, and K. Wodkiewicz, Phys. Rev. A **41**, 369 (1990); **41**, 381 (1990).
[7] See, for example, C. H. Henry, J. Lightwave Technol. **LT-4**, 288 (1986); **LT-4**, 298 (1986).
[8] S. Prasad, Opt. Commun. **85**, 227 (1991).
[9] A. G. Fox and T. Li, Bell Syst. Tech. J. **40**, 453 (1961).
[10] R. Lang, M. O. Scully, and W. E. Lamb Jr., Phys. Rev. A **1**, 1788 (1973).
[11] R. Lang and M. O. Scully, Opt. Commun. **9**, 331 (1973).
[12] K. Ujihara, Phys. Rev. A **12**, 148 (1975); Jpn. J. Appl. Phys. **15**, 1529 (1976); Phys. Rev. A **16**, 562 (1977).
[13] W. H. Louisell, A. Yariv, and A. E. Siegman, Phys. Rev. **124**, 1646 (1961).
[14] B. Mollow and R. J. Glauber, Phys. Rev. **160**, 1076 (1967).
[15] L.-A. Wu and H. J. Kimble, J. Opt. Soc. Am. B **2**, 697 (1985).
[16] C. M. Caves and B. L. Schumaker, Phys. Rev. A **31**, 3068 (1985).
[17] B. Yurke, Phys. Rev. A **32**, 300 (1985).